ACS chemical biology

Letters

Cite This: ACS Chem. Biol. 2019, 14, 4−10

pubs.acs.org/acschemicalbiology

An Isotope-Coded Photocleavable Probe for Quantitative Profiling of Protein *O*-GlcNAcylation

Jingchao Li,[†,◆] Zhonghua Li,[†,◆] Xiaotao Duan,[‡] Ke Qin,[§] Liuyi Dang,[▽] Shisheng Sun,[▽] Li Cai,[#] Linda C. Hsieh-Wilson,[∞] Liming Wu,[*,⊥] and Wen Yi[*,†,⊥]

[†]MOE Laboratory of Biosystems Homeostasis & Protection, College of Life Sciences, Zhejiang University, Hangzhou 310058, China

[‡]State Key Laboratory of Toxicology and Medical Countermeasures, Beijing Institute of Pharmacology and Toxicology, Beijing 100850, China

[§]College of Chemistry and Molecular Engineering, Peking University, Beijing 100871, China

[▽]College of Life Sciences, Northwest University, Xi'an 710069, China

[#]Department of Chemistry, University of South Carolina−Lancaster, Lancaster, South Carolina 29729, United States

[∞]Division of Chemistry and Chemical Engineering, California Institute of Technology, Pasadena, California 91125, United States

[⊥]The First Affiliated Hospital, School of Medicine, Zhejiang University, Hangzhou 310003, China

Supporting Information

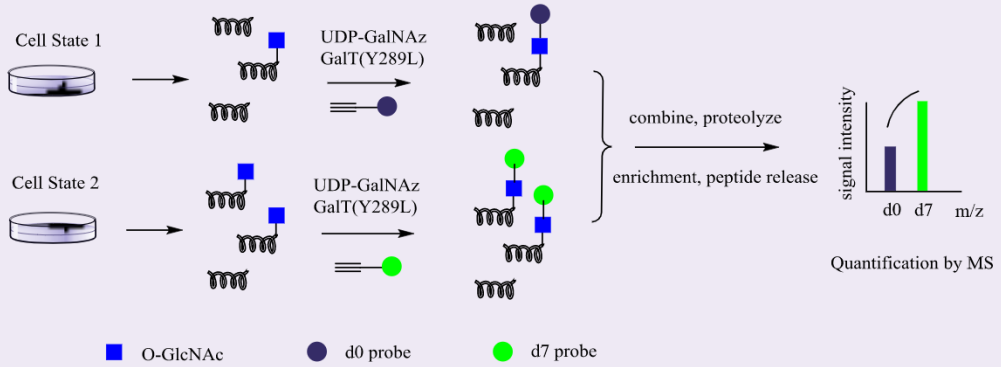

ABSTRACT: *O*-linked *N*-acetylglucosamine (*O*-GlcNAc) is a ubiquitous post-translational modification of proteins and is essential for cell function. Quantifying the dynamics of *O*-GlcNAcylation in a proteome-wide level is critical for uncovering cellular mechanisms and functional roles of *O*-GlcNAcylation in cells. Here, we develop an isotope-coded photocleavable probe for profiling protein *O*-GlcNAcylation dynamics using quantitative mass spectrometry-based proteomics. This probe enables selective tagging and isotopic labeling of *O*-GlcNAcylated proteins in one step from complex cellular mixtures. We demonstrate the application of the probe to quantitatively profile *O*-GlcNAcylation sites in 293T cells upon chemical induction of *O*-GlcNAc levels. We further applied the probe to quantitatively analyze the stoichiometry of *O*-GlcNAcylation between sorafenib-sensitive and sorafenib-resistant liver cancer cells, which lays the foundation for mechanistic investigation of *O*-GlcNAcylation in regulating cancer chemoresistance. Thus, this probe provides a powerful tool to profile *O*-GlcNAcylation dynamics in cells.

Numerous nuclear, mitochondrial, and cytoplasmic proteins are found to be putative glycoproteins containing *O*-GlcNAcylation on serine/threonine residues.[1] *O*-GlcNAcylation is dynamically recycled on proteins through the action of *O*-GlcNAc transferase (OGT) that adds the modification, and *O*-GlcNAcase (OGA) that removes the modification.[2] Recent studies have shown that *O*-GlcNAcylation also occurs on epidermal growth factor (EGF)-like repeats of some membrane and secreted proteins, catalyzed by the EGF domain-specific OGT (EOGT).[3,4] *O*-GlcNAcylation plays a pivotal role in regulating diverse biological processes, including gene expression, neuronal activity, immune response, and disease progression.[5−8] Importantly, analogous to phosphorylation, *O*-GlcNAcylation is reversible and inducible in response to cellular stimuli.[9,10] Moreover, evidence suggests that dynamic *O*-GlcNAcylation is a key mechanism for the spatial and temporal control of the structure and function of proteins.[11−14] Site-specific *O*-GlcNAcylation has demonstrated to govern the biological function of protein substrates.[15−17] Thus, understanding the roles of *O*-GlcNAcylation in specific physiological contexts requires the development of tools to monitor and quantify the dynamics of *O*-GlcNAcylation in a comprehensive manner.

Received: December 4, 2018
Accepted: January 4, 2019
Published: January 8, 2019

DOI: 10.1021/acschembio.8b01052
ACS Chem. Biol. 2019, 14, 4−10

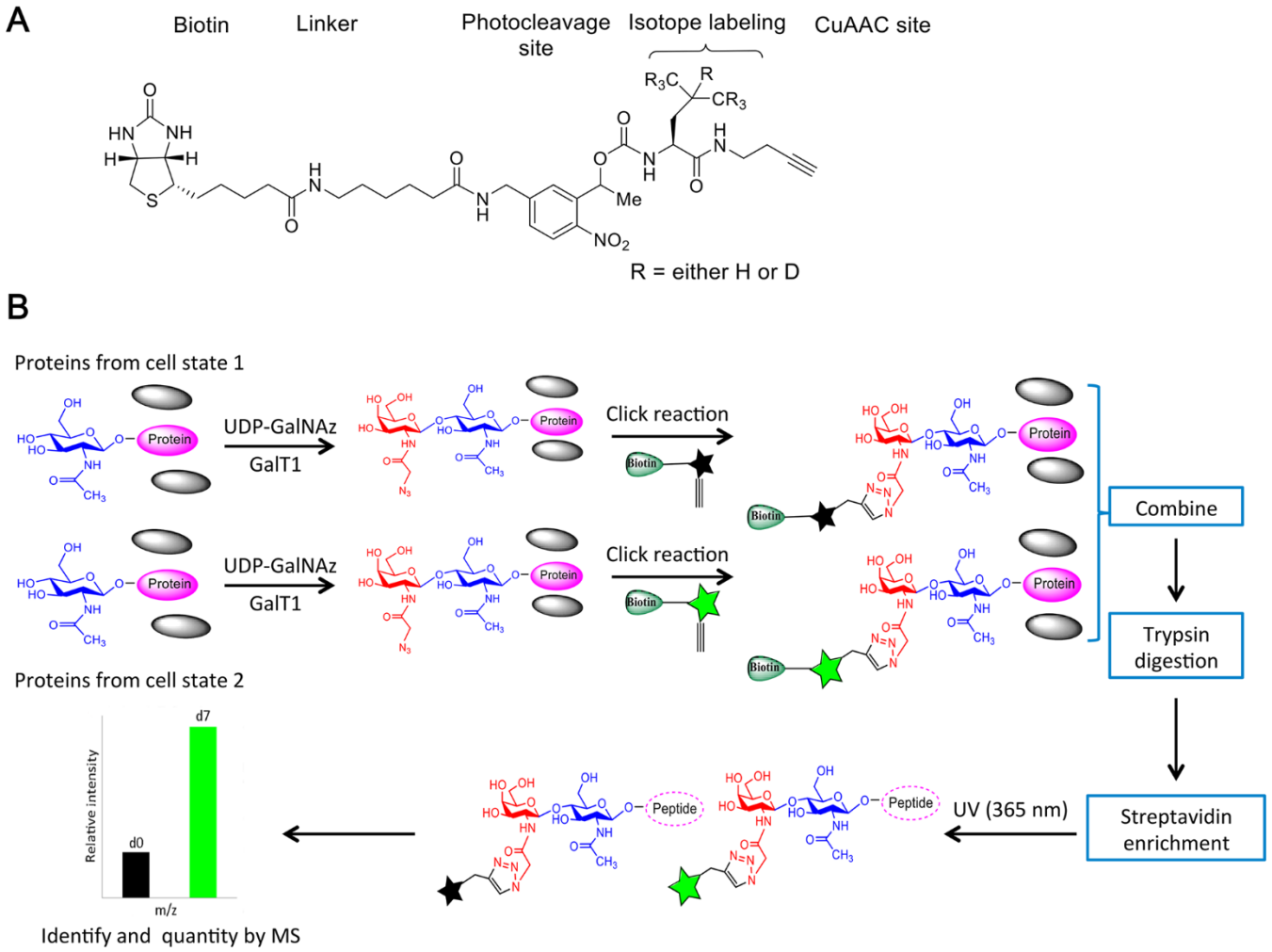

Figure 1. Quantitative profiling of protein *O*-GlcNAcylation using an isotope-coded photocleavable probe: (A) structural design of the isotope-coded photocleavable probe, and (B) strategy for differential labeling and quantitative analysis of *O*-GlcNAcylated proteins.

Current methods for profiling protein *O*-GlcNAcylation includes metabolic labeling of cells with a variety of synthetic GlcNAc analogues,[18−20] and chemo-enzymatic tagging of *O*-GlcNAc with unnatural uridine diphosphate (UDP) sugars.[21−23] The chemo-enzymatic tagging method consists of installation of an unnatural sugar containing a bio-orthogonal functionality onto GlcNAc, and subsequent derivatization with a reporter molecule using click chemistry. Notably, the concept of chemo-enzymatic tagging has been applied in the specific labeling and detection of many different glycan structures besides *O*-GlcNAc.[23−25]

Mass spectrometry-based quantitative proteomics have recently emerged as a powerful tool to quantify phosphorylation or protein expression levels in response to cellular stimuli. Two of the most widely used quantitative proteomics methods, SILAC (Stable Isotope Labeling with Amino Acids in Cell Culture) and iTRAQ (isobaric tags for relative and absolute quantification), coupled with established *O*-GlcNAc peptide enrichment methods (metabolic labeling or chemo-enzymatic tagging), have been successfully applied in the quantification of protein *O*-GlcNAcylation in certain contexts.[26,27] One of the key limitations of these methods is that *O*-GlcNAcylated peptide enrichment and isotopic labeling are separate processes, leading to lengthy sample preparation and possible loss of detection signals.

Inspired by the isotope-targeted proteomics strategy (IsoTaG) established by the Bertozzi group,[28] and the isotopic tandem orthogonal proteolysis-activity-based protein profiling strategy,[29] herein we designed an isotope-coded photocleavable probe for quantitative profiling of *O*-GlcNAcylation (Figure 1A). This probe consists of a biotin affinity handle and alkynl functional group for click chemistry-based affinity enrichment of *O*-GlcNAcylated proteins, a photocleavable linker for facile and efficient release of glycopeptides, and a stable isotope-coded group for differential labeling and quantification of glycosylation sites by mass spectrometry (see the Supporting Information for detailed synthesis). We envision that this probe enables selective tagging/enrichment and isotopic labeling of *O*-GlcNAcylated proteins in one step from complex cellular mixtures (Figure 1B). Specifically, *O*-GlcNAcylated proteins from two cell states (e.g., stimulated versus unstimulated) are chemo-enzymatically tagged with GalNAz and subsequently derivatized with the isotope-coded probes. Tagged glycoproteins are combined, proteolytically digested in solution, and the glycopeptides are further captured on streptavidin beads. The beads are then washed extensively to remove nonspecifically bound peptides and exposed to UV light (365 nm). This results in photocleavage of the linker and obviates the need for a bulky biotin moiety. Recovered

DOI: 10.1021/acschembio.8b01052
ACS Chem. Biol. 2019, 14, 4−10

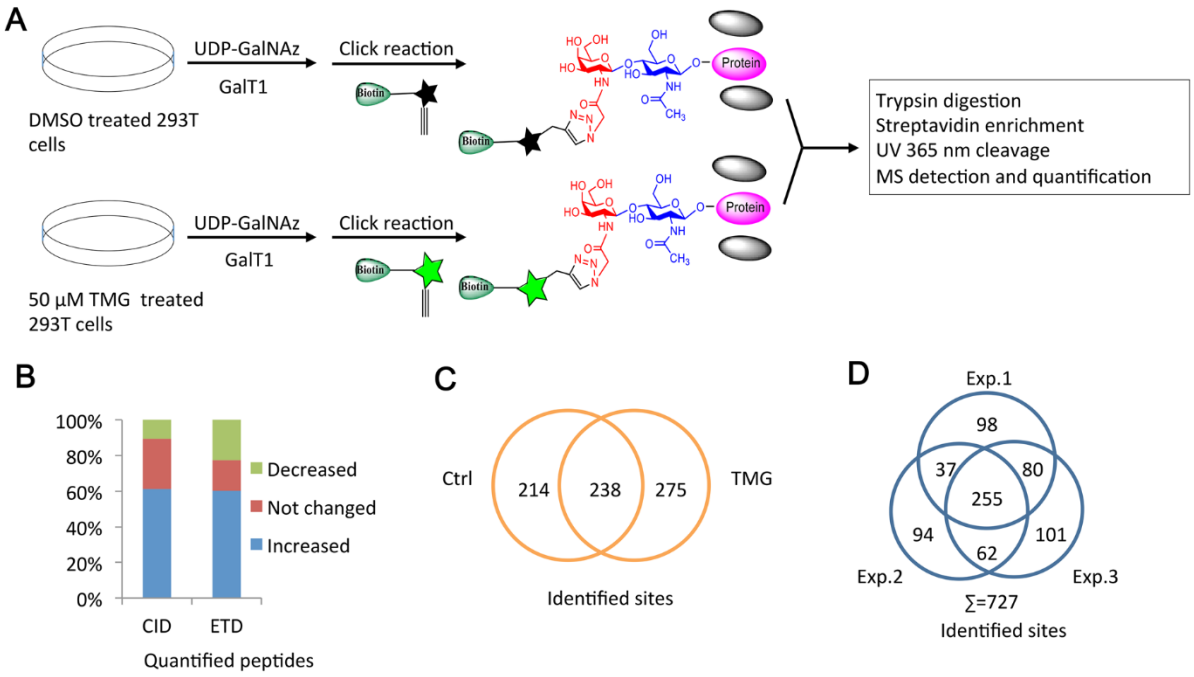

Figure 2. Quantitative profiling of *O*-GlcNAcylation sites in 293T cells upon chemical induction with TMG: (A) 293T cells were treated with or without 50 μM TMG for 12 h, and the cell lysates were chemoenzymatically tagged with GalNAz and further reacted with the $^{1}\mathbf{H}_{7}$ coded and $^{2}\mathbf{D}_{7}$ coded probes, respectively. The "light" and "heavy" samples were mixed, proteolytically digested, capture and analyzed by LC-MS/MS. (B) Distribution of quantified *O*-GlcNAc peptides in 293T cells by CID and ETD. (C) Unambiguously identified *O*-GlcNAc sites in control and TMG-treated 293T cells by ETD. (D) Overlapping of ETD-identified *O*-GlcNAc sites from three biological replicates.

glycopeptides are then analyzed by mass spectrometry for glycosylation site identification and relative quantification.

We first investigated the labeling and quantification of a model *O*-GlcNAcylated peptide. The commercially available peptide TAPT(gS)TIAPG, where gS is *O*-GlcNAcylated, was chemo-enzymatically tagged with GalNAz and the isotope-coded probes. The isotopically labeled peptides were combined, affinity captured, and subjected to UV photo-cleavage (Figure S1A in the Supporting Information). We monitored the reaction progress using liquid chromatography, and performed relative quantification of *O*-GlcNAcylated peptide pairs using mass spectrometry (Figures S1B and S1C in the Supporting Information). Both deuterated and non-deuterated peptides exhibited comparable signal intensities. Glycopeptides were further analyzed with electron-transfer/higher-energy collision dissociation (EThcD) fragmentation tandem mass spectrometry (Figure S2 in the Supporting Information). Higher-energy collision dissociation (HCD) resulted in characteristic loss of tagged GlcNAc moiety and the corresponding oxonium ions (349.2 Da, 427.2 Da for "light" ($^{1}\mathbf{H}_{7}$) labeled, and 356.2 Da, 434.3 Da for "heavy" ($^{2}\mathbf{D}_{7}$) labeled), which allowed for identification of *O*-GlcNAcylated peptides with high confidence (Figure S2). Electron transfer dissociation (ETD) preserved the labile *O*-glycosidic linkage on peptides, thus allowing for the unambiguous identification of the modification sites (Figure S2). Thus, our strategy is validated using the purified glycopeptide.

We next applied the strategy to profile *O*-GlcNAcylated proteins in the cellular level. We modulated global *O*-GlcNAcylation levels in 293T cells with ThiaMet-G (TMG), which is a specific small-molecule inhibitor of OGA.[30] Expectedly, TMG significantly enhanced the overall levels of *O*-GlcNAcylation in cells, as shown by immunoblotting with a pan-anti-*O*-GlcNAc antibody (Figure S3 in the Supporting Information). Cells stimulated with or without TMG were lysed and treated as outlined previously (Figure 2). We analyzed the released peptides by both CID and ETD fragmentation-based MS/MS. (For high confidence peptide identification, we set a peptide score of >10 in CID experiments, and a peptide score of >60 and a delta score of >8 in ETD experiments). CID and ETD identified 406 and 620 *O*-GlcNAcylated peptides, respectively. When conducting relative quantification, we noticed that deuterium could cause small but noticeable shifts in the chromatography profile. However, the elution difference did not convolute the quantification, as shown in the example (Figure 3). The normalized peak-area ratios of differentially mass-tagged peptide pairs were used to measure the relative levels of glycosylation on specific peptides. We quantified 142 and 198 glycopeptides from at least two replicate experiments using CID- and ETD-based MS/MS, respectively (Table S1 in the Supporting Information). More than 60% of the quantified peptides were upregulated in *O*-GlcNAcylation upon TMG treatment in both CID- and ETD-based mass spectra (Figure 2B). Taken together, 130 peptides (corresponding to 95 proteins) exhibited at least a 1.5-fold increase in *O*-GlcNAcylation upon TMG treatment (Table S1). Interestingly, we found that TMG treatment did not result in universal upregulation of *O*-GlcNAcylation on peptides. Decreased glycosylation was found on 65 peptides, and 71 peptides showed no measurable changes in glycosylation (Table S1). These results are in agreement with previous reports, suggesting that regulation of *O*-GlcNAcylation dynamics is dependent on protein and site.[9,30] This also highlights the complex regulatory mechanism of *O*-GlcNAcylation in cells.

To further confirm the quantitative results from mass spectrometry, we biochemically analyzed the changes of *O*-

DOI: 10.1021/acschembio.8b01052
ACS Chem. Biol. 2019, 14, 4−10

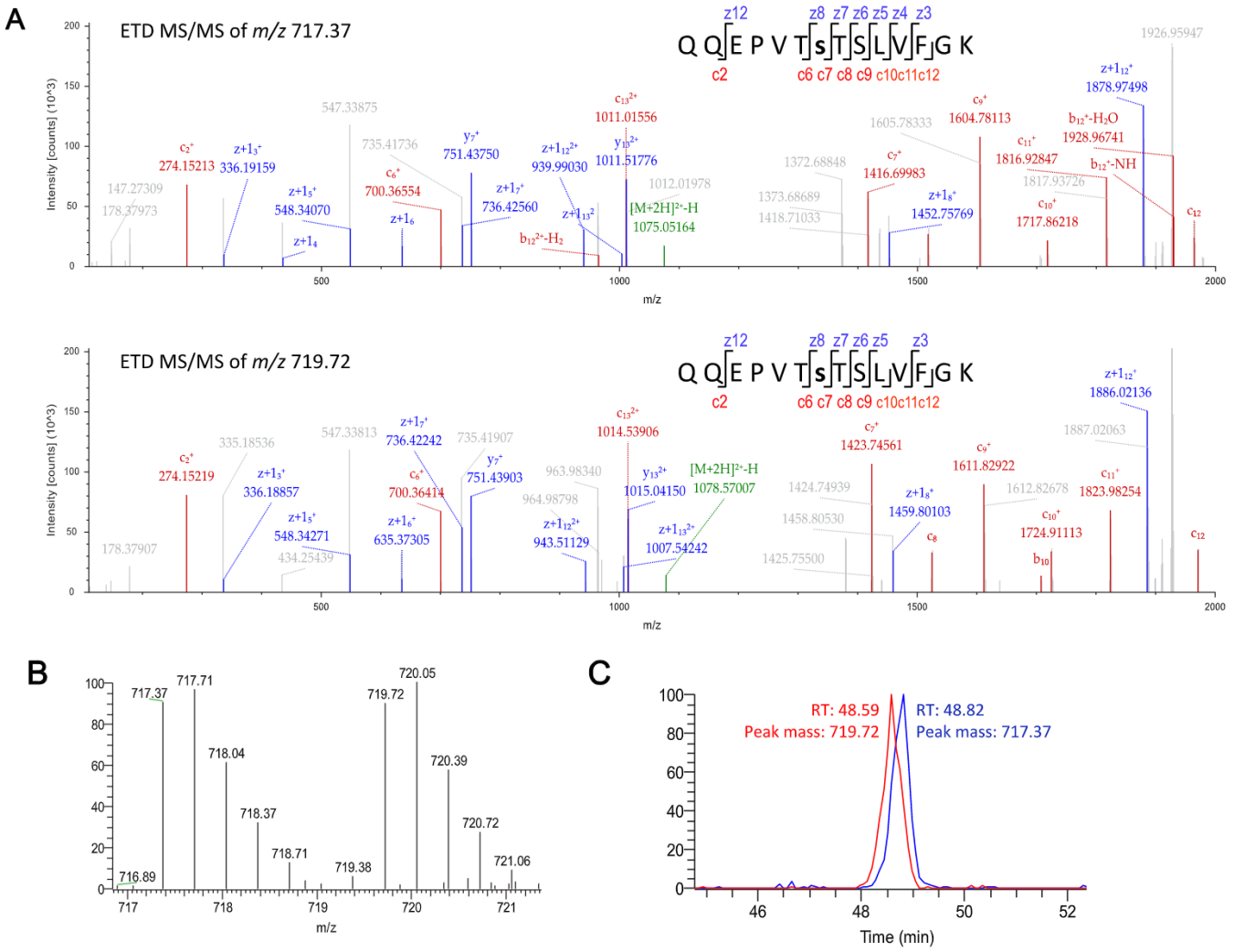

Figure 3. MS spectra and extracted ion chromatogram pair of $^{1}H_{7}$-coded and $^{2}D_{7}$-coded peptide from 293T cells. (A) Representative ETD MS2 spectra of $^{1}H_{7}$-coded (above) and $^{2}D_{7}$-coded (below) *O*-GlcNAc peptide (QQEPVT**s**TSLVFGK, where **s**7 is *O*-GlcNAcylated). This *O*-GlcNAc peptide belongs to Nup153. (B) MS1 spectra of $^{1}H_{7}$-coded and $^{2}D_{7}$-coded *O*-GlcNAc peptide pair are shown. A mass shift of 7 Da between $^{1}H_{7}$-coded and $^{2}D_{7}$-coded peptides was observed ($z = 3$). (C) Extracted ion chromatogram (XIC) of $^{1}H_{7}$-coded (blue) and $^{2}D_{7}$-coded (red) peptides.

GlcNAcylation on a few selected proteins. Specifically, *O*-GlcNAcylated proteins from cell lysates treated with or without TMG were chemoenzymatically tagged and conjugated with traditional biotin-containing probes.[14] Following affinity capture and elution, the eluents were immunoblotted with antibodies for specific proteins and the changes in *O*-GlcNAcylation were quantified based on the relative amounts of proteins released from the affinity beads (Figure S4 in the Supporting Information). We observed that *O*-GlcNAcylation was induced by ~5-fold on E3 ubiquitin-protein ligase (CBL), ~1.5-fold on lysine-specific demethylase 3B (KDM3B), and ~2-fold on Arf-GAP domain and FG repeat-containing protein 1 (AGFG1), consistent with the results obtained from the proteomic approach (Figure S4).

With ETD fragmentation, we identified 452 and 513 *O*-GlcNAcylation sites with high confidence from control and TMG-treated 293T cells, respectively (Table S2 in the Supporting Information). Among them, 238 sites contained both "light" and "heavy" labels (Figure 2C), and 434 sites were identified from at least two replicates (Figure 2D). When compared with previous studies, we found that a total of 370 sites were newly identified in this work (Table S2). Tandem mass spectra of two representative *O*-GlcNAcylated peptides were shown (Figure S5 in the Supporting Information). In order to further validate the site mapping results, we performed site-directed mutagenesis on the putative glycosylation sites. We observed that mutating the glycosylation site residues (serine or threonine) to alanine significantly reduced the glycosylation level of the mutant protein, compared to the wild-type (Figure S5), confirming the site identification by MS. However, site mutations did not totally abolish glycosylation, suggesting the existence of other glycosylation sites not being identified from the proteomic study. This is not unexpected, because the complexity of peptide mixtures might compromise the efficiency of peptide backbone fragmentation. Nevertheless, these results validated our approach in the identification of the glycosylation sites.

Having demonstrated the utility of our strategy to probe the reversibility of *O*-GlcNAcylation in cells, we next applied our strategy to profile *O*-GlcNAcylation under a more physiological context. Increasing evidence suggests that aberrant expression of *O*-GlcNAcylation contributes to the development and progression of a variety of diseases.[5,14,15,26,31] Drug resistance developed during cancer chemotherapy constitutes

DOI: 10.1021/acschembio.8b01052
ACS Chem. Biol. 2019, 14, 4−10

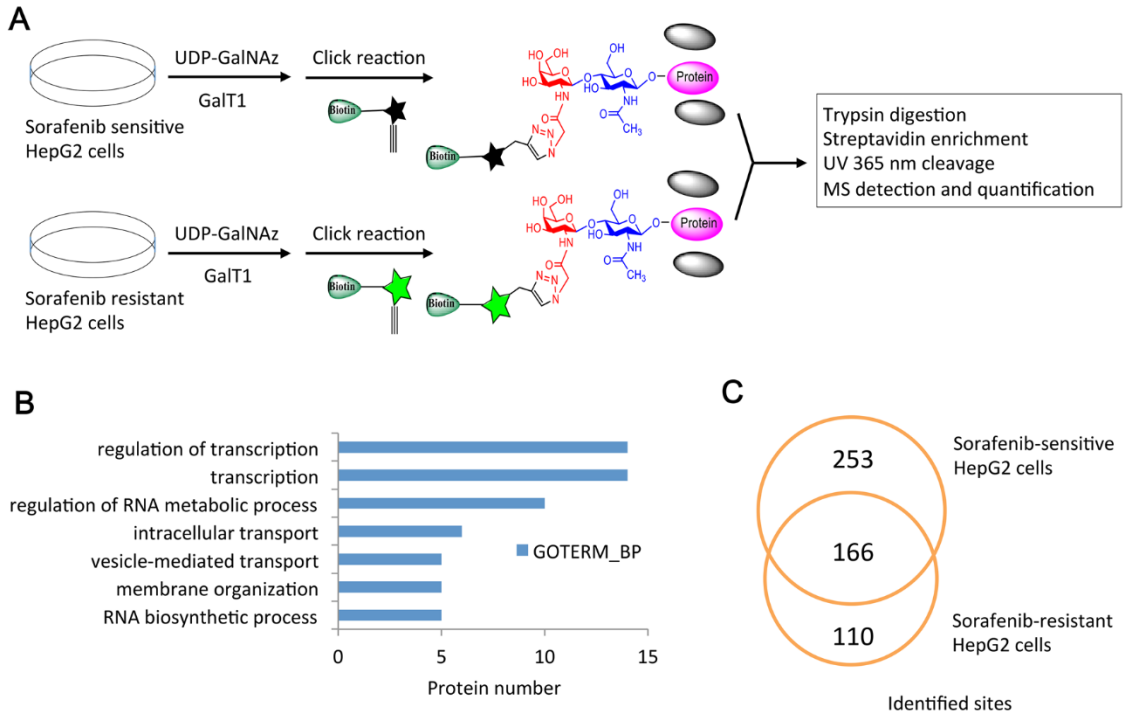

Figure 4. Quantitative analysis of *O*-GlcNAcylation sites in sorafenib-sensitive and sorafenib-resistant HepG2 cells. (A) Cell lysates from sorafenib-sensitive and sorafenib-resistant HepG2 cells were chemo-enzymatically tagged, reacted with isotope-coded probes, mixed, digested, enriched, and analyzed by LC-MS/MS. (B) GO analysis of proteins with more than 1.2-fold increase in *O*-GlcNAcylation stoichiometry, compared with the sensitive cells. (C) The number of identified *O*-GlcNAc sites from sorafenib-sensitive and sorafenib-resistant HepG2 cells with ETD-based MS/MS.

an important obstacle that compromises the treatment effectiveness. *O*-GlcNAcylation has emerged as an important mechanism in regulating gene transcription, cell proliferation, apoptosis, and cell survival. However, its role in regulating drug resistance has been largely unexplored. We aimed to apply our quantitative proteomic strategy to identify key substrates of *O*-GlcNAcylation that may play an important role in regulating drug resistance in cancer cells. We showed that global *O*-GlcNAcylation levels were dramatically different between paired drug-sensitive and drug-resistant cell lines (Figure S6 in the Supporting Information). We chose to investigate the liver cancer cell line HepG2 and the corresponding sorafenib-resistant cell line. *O*-GlcNAcylated proteins from these two cell populations were chemo-enzymatically labeled, conjugated with the isotope-coded probes, and subjected to further treatment as described previously (Figure 4). A total of 94 and 150 *O*-GlcNAcylated peptides were quantified from at least two replicates, via CID and ETD, respectively (Table S3 in the Supporting Information). A total of 55 peptides in the sorafenib-resistant cells possessed at least a 1.2-fold increase in *O*-GlcNAcylation stoichiometry, compared with the sensitive cells. They were distributed on 47 proteins, which were significantly enriched in biological processes, such as gene transcription and regulation of transcription (Figure 4B). In contrast, 136 peptides (corresponding to 105 proteins) in the resistant cells possessed at least a 1.2-fold decrease in *O*-GlcNAcylation stoichiometry, compared to the sensitive cells (Table S3). From sorafenib-sensitive and sorafenib-resistant HepG2 cells, we identified 419 and 276 *O*-GlcNAcylation sites with high confidence using ETD fragmentation, respectively (Table S4 in the Supporting Information). Among them, 166 sites were overlapped, and 262 sites were novel sites not identified in previous studies (see Figure 4C, as well as Table S4 in the Supporting Information). These data suggested that protein *O*-GlcNAcylation underwent aberrant changes in sorafenib-resistant liver cancer cells, when compared with its sensitive counterparts. It also lays a foundation for uncovering the molecular mechanisms underlying the chemoresistance in liver cancer.

In summary, we have designed and synthesized an isotope-coded photocleavable probe to profile protein *O*-GlcNAcylation sites and dynamics using quantitative proteomics. This probe allows for selective tagging, enrichment, and isotopic labeling of *O*-GlcNAcylated peptides in a facile manner from complex cellular context. With this probe, we quantitatively profile *O*-GlcNAcylation peptides/sites in 293T cells upon chemical induction of *O*-GlcNAc levels, demonstrating that *O*-GlcNAcylation is regulated site-specifically. We further applied the probe to quantitatively analyze the stoichiometry of *O*-GlcNAcylation between sorafenib-sensitive and sorafenib-resistant liver cancer cells, which lays the foundation for mechanistic investigation of *O*-GlcNAcylation in regulating cancer chemoresistance. Thus, this probe provides a powerful tool to profile the *O*-GlcNAcylation dynamics in cells.

■ ASSOCIATED CONTENT

Supporting Information

The Supporting Information is available free of charge on the ACS Publications website at DOI: 10.1021/acschembio.8b01052.

Details of experimental materials, methods, and supporting figures (PDF)

Data set of quantified glycopeptides from 293T cells (XLSX)

DOI: 10.1021/acschembio.8b01052
ACS Chem. Biol. 2019, 14, 4−10

Data set of identified *O*-GlcNAcylation sites from 293T cells (XLSX)

Data set of quantified glycopeptides from HepG2 cells (XLSX)

Data set of identified *O*-GlcNAcylation sites from HepG2 cells (XLSX)

AUTHOR INFORMATION

Corresponding Authors

*E-mail: wlm@zju.edu.cn (L. Wu).

*E-mail: wyi@zju.edu.cn (W. Yi).

ORCID

Li Cai: 0000-0002-6098-1168

Linda C. Hsieh-Wilson: 0000-0001-5661-1714

Wen Yi: 0000-0002-4257-3355

Author Contributions

◆These authors contributed equally to this work.

Notes

The authors declare no competing financial interest.

ACKNOWLEDGMENTS

This work was supported by the National Science Foundation of China (NSFC, Grant Nos. 91753125, 31322019, 31570804, and 81673387), the National Key Research and Development Program of China (No. 2016YFA0100303), Beijing Nova Program (No. Z161100004916163), and the National Science Foundation of Zhejiang Province (No. LR15C050001).

REFERENCES

(1) Peterson, S. B., and Hart, G. W. (2016) New insights: A role for *O*-GlcNAcylation in diabetic complications. *Crit. Rev. Biochem. Mol. Biol. 51*, 150−161.

(2) Vocadlo, D. J. (2012) *O*-GlcNAc processing enzymes: catalytic mechanisms, substrate specificity, and enzyme regulation. *Curr. Opin. Chem. Biol. 16*, 488−497.

(3) Tashima, Y., and Stanley, P. (2014) Antibodies that detect O-linked *β*-D-N-acetylglucosamine on the extracellular domain of cell surface glycoproteins. *J. Biol. Chem. 289*, 11132−11142.

(4) Alfaro, J. F., Gong, C. X., Monroe, M. E., Aldrich, J. T., Clauss, T. R., Purvine, S. O., Wang, Z., Camp, D. G., 2nd., Shabanowitz, J., Stanley, P., Hart, G. W., Hunt, D. F., Yang, F., and Smith, R. D. (2012) Tandem mass spectrometry identifies many mouse brain *O*-GlcNAcylated proteins including EGF domain-specific *O*-GlcNAc transferase targets. *Proc. Natl. Acad. Sci. U. S. A. 109*, 7280−7285.

(5) Hart, G. W., Slawson, C., Ramirezcorrea, G., and Lagerlof, O. (2011) Cross talk between O-glcnacylation and phosphorylation: roles in signaling, transcription, and chronic disease. *Annu. Rev. Biochem. 80*, 825−858.

(6) Rexach, J. E., Clark, P. M., Mason, D. E., Neve, R. L., Peters, E. C., and Hsieh-Wilson, L. C. (2012) Dynamic *O*-GlcNAc modification regulates CREB-mediated gene expression and memory formation. *Nat. Chem. Biol. 8*, 253−261.

(7) Swamy, M., Pathak, S., Grzes, K. M., Damerow, S., Sinclair, L. V., van Aalten, D. M., and Cantrell, D. A. (2016) Glucose and glutamine fuel protein *O*-GlcNAcylation to control T cell self-renewal and malignancy. *Nat. Immunol. 17*, 712−720.

(8) Ferrer, C. M., Sodi, V. L., and Reginato, M. J. (2016) *O*-GlcNAcylation in cancer biology: linking metabolism and signaling. *J. Mol. Biol. 428*, 3282−3294.

(9) Leney, A. C., El Atmioui, D., Wu, W., Ovaa, H., and Heck, A. J. R. (2017) Elucidating crosstalk mechanisms between phosphorylation and *O*-GlcNAcylation. *Proc. Natl. Acad. Sci. U. S. A. 114*, E7255−E7261.

(10) Zachara, N. E., O'Donnell, N., Cheung, W. D., Mercer, J. J., Marth, J. D., and Hart, G. W. (2004) Dynamic *O*-GlcNAc modification of nucleocytoplasmic proteins in response to stress. A survival response of mammalian cells. *J. Biol. Chem. 279*, 30133−30142.

(11) Chuh, K. N., Batt, A. R., Zaro, B. W., Darabedian, N., Marotta, N. P., Brennan, C. K., Amirhekmat, A., and Pratt, M. R. (2017) The new chemical reporter 6-alkynyl-6-deoxy-glcnac reveals *O*-GlcNAc modification of the apoptotic caspases that can block the cleavage/activation of caspase-8. *J. Am. Chem. Soc. 139*, 7872−7885.

(12) Lazarus, M. B., Jiang, J., Kapuria, V., Bhuiyan, T., Janetzko, J., Zandberg, W. F., Vocadlo, D. J., Herr, W., and Walker, S. (2013) HCF-1 is cleaved in the active site of *O*-GlcNAc transferase. *Science 342*, 1235−1239.

(13) Andres, L. M., Blong, I. W., Evans, A. C., Rumachik, N. G., Yamaguchi, T., Pham, N. D., Thompson, P., Kohler, J. J., and Bertozzi, C. R. (2017) Chemical modulation of protein *O*-GlcNAcylation via OGT inhibition promotes human neural cell differentiation. *ACS Chem. Biol. 12*, 2030−2039.

(14) Rao, X., Duan, X., Mao, W., Li, X., Li, Z., Li, Q., Zheng, Z., Xu, H., Chen, M., Wang, P. G., Wang, Y., Shen, B., and Yi, W. (2015) *O*-GlcNAcylation of G6PD promotes the pentose phosphate pathway and tumor growth. *Nat. Commun. 6*, 8468.

(15) Shin, H., Cha, H. J., Na, K., Lee, M. J., Cho, J. Y., Kim, C. Y., Kim, E. K., Kang, C. M., Kim, H., and Paik, Y. K. (2018) *O*-GlcNAcylation of the tumor suppressor FOXO3 triggers aberrant cancer cell growth. *Cancer Res. 78*, 1214−1224.

(16) Han, C., Gu, Y., Shan, H., Mi, W., Sun, J., Shi, M., Zhang, X., Lu, X., Han, F., Gong, Q., and Yu, W. (2017) *O*-GlcNAcylation of SIRT1 enhances its deacetylase activity and promotes cytoprotection under stress. *Nat. Commun. 8*, 1491.

(17) Peng, C., Zhu, Y., Zhang, W., Liao, Q., Chen, Y., Zhao, X., Guo, Q., Shen, P., Zhen, B., Qian, X., Yang, D., Zhang, J. S., Xiao, D., Qin, W., and Pei, H. (2017) Regulation of the Hippo-YAP pathway by glucose sensor *O*-GlcNAcylation. *Mol. Cell 68*, 591−604.

(18) Vocadlo, D. J., Hang, H. C., Kim, E. J., Hanover, J. A., and Bertozzi, C. R. (2003) A chemical approach for identifying *O*-GlcNAc-modified proteins in cells. *Proc. Natl. Acad. Sci. U. S. A. 100*, 9116−9121.

(19) Zaro, B. W., Yang, Y. Y., Hang, H. C., and Pratt, M. R. (2011) Chemical reporters for fluorescent detection and identification of *O*-GlcNAc-modified proteins reveal glycosylation of the ubiquitin ligase NEDD4−1. *Proc. Natl. Acad. Sci. U. S. A. 108*, 8146−8151.

(20) Tan, H. Y., Eskandari, R., Shen, D., Zhu, Y., Liu, T. W., Willems, L. I., Alteen, M. G., Madden, Z., and Vocadlo, D. J. (2018) Direct one-step fluorescent labeling of *O*-GlcNAc-modified proteins in live cells using metabolic intermediates. *J. Am. Chem. Soc. 140*, 15300−15308.

(21) Khidekel, N., Arndt, S., Lamarre-Vincent, N., Lippert, A., Poulin-Kerstien, K. G., Ramakrishnan, B., Qasba, P. K., and Hsieh-Wilson, L. C. (2003) A chemoenzymatic approach toward the rapid and sensitive detection of *O*-GlcNAc posttranslational modifications. *J. Am. Chem. Soc. 125*, 16162−16163.

(22) Darabedian, N., Thompson, J. W., Chuh, K. N., Hsieh-Wilson, L. C., and Pratt, M. R. (2018) Optimization of chemoenzymatic mass tagging by strain-promoted cycloaddition (SPAAC) for the determination of *O*-GlcNAc stoichiometry by western blotting. *Biochemistry 57*, 5769−5774.

(23) Lopez Aguilar, A., Briard, J. G., Yang, L., Ovryn, B., Macauley, M. S., and Wu, P. (2017) Tools for studying glycans: recent advances in chemoenzymatic glycan labeling. *ACS Chem. Biol. 12*, 611−621.

(24) Sun, T., Yu, S. H., Zhao, P., Meng, L., Moremen, K. W., Wells, L., Steet, R., and Boons, G. J. (2016) One-step selective exoenzymatic labeling (SEEL) strategy for the biotinylation and identification of glycoproteins of living cells. *J. Am. Chem. Soc. 138*, 11575−11582.

(25) Wen, L., Zheng, Y., Jiang, K., Zhang, M., Kondengaden, S. M., Li, S., Huang, K., Li, J., Song, J., and Wang, P. G. (2016) Two-step chemoenzymatic detection of N-acetylneuraminic acid-*α*(2−3)-galactose glycans. *J. Am. Chem. Soc. 138*, 11473−11476.

(26) Qin, W., Lv, P., Fan, X., Quan, B., Zhu, Y., Qin, K., Chen, Y., Wang, C., and Chen, X. (2017) Quantitative time-resolved chemo-

DOI: 10.1021/acschembio.8b01052
ACS Chem. Biol. 2019, 14, 4−10

proteomics reveals that stable *O*-GlcNAc regulates box C/D snoRNP biogenesis. *Proc. Natl. Acad. Sci. U. S. A. 114*, E6749−E6758.
(27) Tsumoto, H., Akimoto, Y., Endo, T., and Miura, Y. (2017) Quantitative analysis of *O*-GlcNAcylation in combination with isobaric tag labeling and chemoenzymatic enrichment. *Bioorg. Med. Chem. Lett. 27*, 5022−5026.
(28) Woo, C. M., Iavarone, A. T., Spiciarich, D. R., Palaniappan, K. K., and Bertozzi, C. R. (2015) Isotope-targeted glycoproteomics (isotag): a mass-independent platform for intact N- and O-glycopeptide discovery and analysis. *Nat. Methods 12*, 561−567.
(29) Weerapana, E., Wang, C., Simon, G. M., Richter, F., Khare, S., Dillon, M. B., Bachovchin, D. A., Mowen, K., Baker, D., and Cravatt, B. F. (2010) Quantitative reactivity profiling predicts functional cysteines in proteomes. *Nature 468*, 790−795.
(30) Khidekel, N., Ficarro, S. B., Clark, P. M., Bryan, M. C., Swaney, D. L., Rexach, J. E., Sun, Y. E., Coon, J. J., Peters, E. C., and Hsieh-Wilson, L. C. (2007) Probing the dynamics of *O*-GlcNAc glycosylation in the brain using quantitative proteomics. *Nat. Chem. Biol. 3*, 339−348.
(31) Wang, S., Yang, F., Petyuk, V. A., Shukla, A. K., Monroe, M. E., Gritsenko, M. A., Rodland, K. D., Smith, R. D., Qian, W. J., Gong, C. X., and Liu, T. (2017) Quantitative proteomics identifies altered *O*-GlcNAcylation of structural, synaptic and memory-associated proteins in Alzheimer's disease. *J. Pathol. 243*, 78−88.

DOI: 10.1021/acschembio.8b01052
ACS Chem. Biol. 2019, 14, 4−10